and temperature dependence of χ_1, χ_2, and χ_3 can provide a good test of any proposed level scheme.

The temperature dependence of the quadrupolar splittings of the Al^{27} resonance lines indicates a change with temperature in the oxygen configurations, probably involving increased distortion of the AlO_4 tetrahedra with increasing temperature. A low-temperature structure study would show what oxygen position changes occur. The unshielded efg at the aluminum sites in several aluminum garnets and at the iron sites in some iron garnets are predicted quite accurately by a point-charge model having charge $3e$ at each trivalent cation site and *positive* charge $1.2e$ at each oxygen site. It would be of interest to see if similar point-charge models for other crystals require positive charges at oxygen sites.

ACKNOWLEDGMENTS

We wish to thank R. J. Baughman for growing the single crystals, Dr. B. Morosin for supplying x-ray structure data in advance of publication, Dr. A. Narath for providing the dipole-sum computer program, and R. R. Knispel for assistance with computer calculations of efg. One of us (V.H.S.) gratefully acknowledges summer support at Sandia Laboratories under the Association of Western Universities Atomic Energy Commission Faculty Participation Program, and thanks personnel at Sandia Laboratories for their hospitality.

PHYSICAL REVIEW B VOLUME 1, NUMBER 5 1 MARCH 1970

Electron Paramagnetic Resonance of V^{3+} Ions in Zinc Oxide

G. FILIPOVICH, A. L. TAYLOR, AND R. E. COFFMAN*
3M Company, Central Research Laboratories, St. Paul, Minnesota 55101
(Received 28 April 1969; revised manuscript received 22 October 1969)

The paramagnetic resonance of trace amounts of V^{3+} in single-crystal hexagonal zinc oxide is reported. The EPR spectrum is fitted with an axially symmetric spin Hamiltonian with five empirically determined parameters: D, $g_{\parallel}$, $g_{\perp}$, A, and B. The spin-Hamiltonian parameters are interpreted in terms of the Racâh parameter B, the crystal-field parameters Dq, Ds, Dt, and the spin-orbit coupling constant λ. The values of these parameters derived from the EPR data are consistent with a model in which the V^{3+} replaces a Zn^{2+} in a trigonally elongated tetrahedral site. This is in agreement with a recent redetermination of the crystallographic unit-cell parameters of ZnO.

I. INTRODUCTION

THE electron-paramagnetic-resonance (EPR) absorption of V^{3+} in tetrahedral site symmetry has been reported for vanadium in ZnS and ZnTe crystals[1,2] having the cubic zinc sulfide structure. The EPR spectrum of V^{3+} in an eightfold coordinated cubic site has been reported for vanadium in single-crystal CaF_2,[3] having the fluorite structure. In both the fourfold and eightfold cubic coordination, the crystal-field potential has the opposite sign in relation to the crystal-field potential for the sixfold octahedral coordination.[4] The ground state is therefore orbitally nondegenerate with a small amount of mixing of excited orbital momentum states due primarily to the spin-orbit coupling. The ground-state spin degeneracy is not removed in these cases, so the EPR spectra are magnetically isotropic for the cases of tetrahedral symmetry.

The EPR[2] and optical spectra[5] of V^{3+} in single-crystal CdS having the zincite (wurtzite) structure have been reported. The Cd site in this crystal structure is axially distorted because the Cd-S distance along the crystalline c axis is shorter than the other three Cd-S separations in the tetrahedron. These distances were believed, in 1948, to be 2.51 and 2.53 Å, respectively.[5,6] In this paper, we present the results of a study of the EPR of V^{3+} in a Zn-atom subsitutional site in single-crystal ZnO. Recently, the atomic distances in ZnO have been remeasured[7] and show a slight axial elongation of the tetrahedron (Fig. 1). The Zn-O c-axis distance is 1.992 Å, while the other three Zn-O bond distances are each 1.973 Å. According to the data published in 1948,[6] these same dimensions are 1.796 and 2.040 Å, respectively, indicating a large axial compression. This c-axis trigonal distortion partially removes the spin degeneracy of the $^3A_{2g}$ ground state, giving anisotropic EPR spec-

* Present address: Chemistry Department, University of Iowa, Iowa City, Ia. 52240.
[1] W. C. Holton, J. Schneider, and T. L. Estle, Phys. Rev. **133**, A1638 (1964).
[2] G. W. Ludwig and H. H. Woodbury, Bull. Am. Phys. Soc. **6**, 118 (1961); Solid State Phys. **13**, 299 (1962).
[3] M. M. Zaripov, V. S. Kropotov, L. D. Livanova, and V. G. Stepanov, Fiz. Tverd. Tela **9**, 209 (1967) [English transl.: Soviet Phys.—Solid State **9**, 155 (1967)].
[4] J. S. Griffith, *The Theory of the Transition Metal Ions* (Cambridge University Press, Cambridge, England, 1961).
[5] R. Pappalardo and R. E. Dietz, Phys. Rev. **123**, 1188 (1961).
[6] R. W. G. Wyckoff, *Crystal Structures* (Wiley-Interscience Inc., 1949), Vol. I, table p. 31.
[7] S. C. Abrahams and J. L. Bernstein, Acta Cryst. **25**, 1233 (1969).

tra. The magnetic anisotropy is much more pronounced for ZnO:V^{3+} than for CdS:V^{3+}, which permits a more detailed analysis of the paramagnetic properties of the impurity center. An electrostatic model for the magnetic anisotropy is developed, which depends explicitly on the axial compression or elongation of the tetrahedron of oxide ions about the V^{3+} ion.

II. EXPERIMENTAL PROCEDURES

ZnO crystals grown in the 3M laboratory by the vapor-phase technique were used for this study. Vanadium was detected in crystals as-grown at concentrations less than 1 ppm by weight by emission spectroscopic analysis. The direction of the hexagonal crystal's c axis with respect to the outside faces was determined by an x-ray diffraction method. The crystals were mounted on a copper rod centered inside a Dewar which in turn was centered inside a rectangular TE_{102} microwave cavity. The angle of the crystal's c axis (rotated in a horizontal plane) with the magnetic field was varied by rotating the copper rod around the vertical axis. In this manner, the microwave magnetic field H_1, remained perpendicular and the modulation field parallel to H_0. The crystal was cooled by having only the upper part of the copper rod submerged in liquid nitrogen. There was no liquid nitrogen in the part of the Dewar containing the crystal inside the cavity. This prevented excessive noise due to bubbling. Use of 100-kc/sec field-modulation frequency provided sufficient signal-to-noise ratio of 77°K at relatively low concentrations of vanadium in the crystals.

Most of the spectra used for evaluation of the angular dependence of the fine and hyperfine structure, as well as intensities, were recorded on a Varian V-4502 EPR spectrometer with 9″ magnet equipped with Fieldial magnetic field regulation and control. Additional resonance measurements for the accurate determination of the spin-Hamiltonian parameters were made on several EPR spectrometers at the School of Chemistry, University of Minnesota, using a Varian F-8 NMR Fluxmeter for magnetic field measurements and a Hewlett Packard model 524D frequency counter with transfer oscillator for accurate determination of the microwave frequency.

III. EXPERIMENTAL RESULTS

The magnetic resonances consisted of sets of hyperfine lines, the centers of which varied isotropically for rotation of $\mathbf{H}_0$ in a plane perpendicular to the c axis, but revealed an extreme anisotropy when $\mathbf{H}_0$ was rotated in a plane which included the c axis. We refer to a single such set of hyperfine lines as a hfs band. One hfs band was detected for $\mathbf{H}_0 \perp c$, but a maximum of three hfs bands could be detected for $\mathbf{H}_0$ 10° away from $\mathbf{H}_0 \| c$. The angular dependence of the fine structure resonances in the XZ plane is shown in Fig. 2. The solid lines are the calculated centers of EPR lines for an $S=1$ system

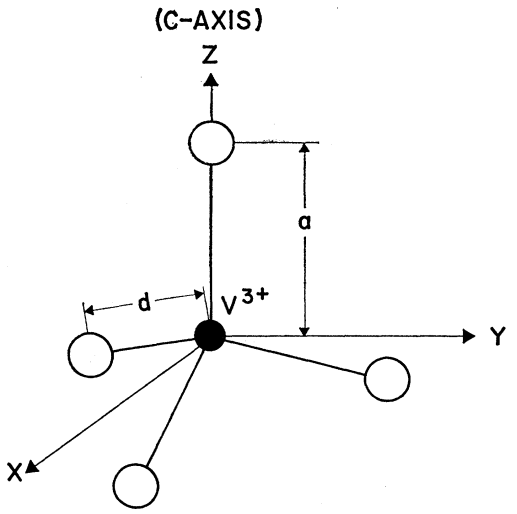

FIG. 1. A vanadium ion substituting for a Zn atom in ZnO. The bond parallel to the c axis is slightly elongated with respect to the other three equidistant bond lengths. This creates a trigonal component of the crystal field.

with zero-field splitting. We were unable to make EPR measurements above 10 000 G because of instrumental field limitations.

Eight hfs lines are observed within the single hfs band measured with $\mathbf{H}_0 \perp c$ [see Fig. 3(a)], but as the direction of H_0 changes between $\mathbf{H}_0 \perp c$ and $\mathbf{H}_0 \| c$ the number of hfs lines varies considerably. At intermediate angles [Fig. 3(b)], up to 44 hfs lines may be counted. As H_0 approaches the c direction, this band becomes very weak and exhibits 15 hfs lines near the point of vanishingly small intensity at $\mathbf{H}_0 \| c$ [Fig. 3(c)]. Within ±16° of $\mathbf{H}_0 \| c$, two other bands are observed, but the extremum point of only one of these was measured. For the spectra recorded at 9.3 gHz these two bands vanish for $|\theta| > 18°$, as illustrated in Fig. 4. For $\mathbf{H}_0 \| c$, the 5000 G band shows 8 hfs lines, as does the single band meaured

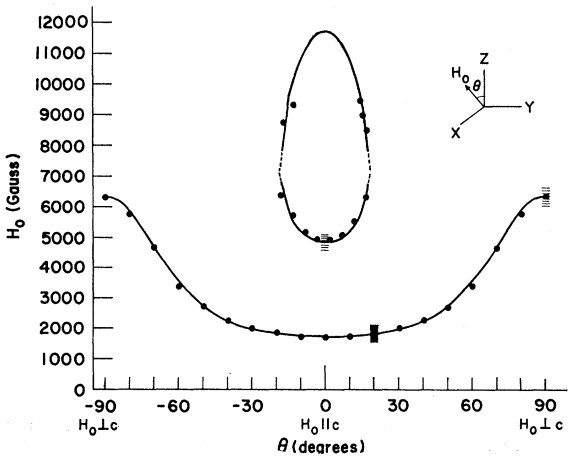

FIG. 2. Angular dependence of the centers of the hyperfine structure bands; $\nu = 9.3$ GHz.

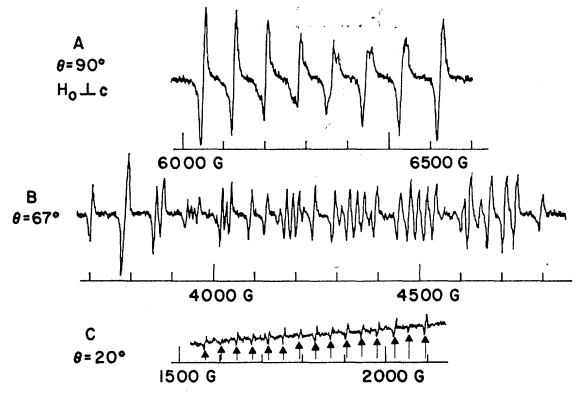

FIG. 3. EPR absorption derivatives; (a) $\mathbf{H}_0 \perp c$ 8 hyperfine lines are observed; (b) $\theta=67°$, at intermediate angles up to 44 lines may be counted, many of them due to "forbidden" ($\Delta m \neq 0$) transitions; (c) $\theta=20°$, 15 lines with weak intensity are observed, seven of which are $\Delta m=\pm 1$ transitions.

for $\mathbf{H}_0 \perp c$. Experiments to measure relative intensities of bands versus temperature with the intension of determining the sign of "D" [Eq. (1)] were unsuccessful because of signal-to-noise problems.

IV. SPIN HAMILTONIAN

An axially symmetric spin Hamiltonian of the following form was used to fit the experimental data:

$$\mathcal{H}=D[S_z^2-\tfrac{1}{3}S(S+1)]+g_{\parallel}\beta H_z S_z+g_{\perp}\beta(H_x S_x+H_y S_y) +AS_zI_z+B(S_xI_x+S_yI_y). \quad (1)$$

Approximate values for $g_{\parallel}$, $g_{\perp}$, and D were first determined by computing the resonance field values, in gauss, and the relative intensities of the EPR transitions within as $S=1$ manifold of spin states using this reduced spin Hamiltonian

$$\mathcal{H}=D(S_z^2-\tfrac{2}{3})+g_{\parallel}\beta H_0 \cos\theta\, S_z+g_{\perp}\beta H_0 \sin\theta\, S_x.$$

The z axis is chosen as the crystalline c axis, and the x axis is any direction perpendicular to the z axis. In this way we obtained a good fit for the centers of the hfs band versus θ in the XZ plane (Fig. 2). Approximations to the values of the hyperfine constants were then obtained by using

$$A \approx g_{\parallel}\beta\langle\Delta H\rangle_{\parallel}, \quad B \approx g_{\perp}\beta\langle\Delta H\rangle_{\perp},$$

where $\langle\Delta H\rangle_{\parallel}$ and $\langle\Delta H\rangle_{\perp}$ are the average hfs splittings for $\mathbf{H}_0 \| c$ and $\mathbf{H}_0 \perp c$, respectively.

Refined values of the spin-Hamiltonian parameters were obtained from accurate resonant field strength and microwave frequency measurements on two of the bands at their extremum points. In the case of $\mathbf{H}_0 \| c$, the lowest-field band (Fig. 2) had to be extrapolated in order to determine the hyperfine line positions at the turning point. The data obtained for $H_0 \| c$ were treated by second-order perturbation theory. From these data, values of $g_{\parallel}$, A, and D were extracted by finding implicit solutions to the perturbation theory eigenvalue equations. By this procedure, it was possible to predict the variation of the hyperfine splitting $\Delta H_{\parallel}$ with nuclear quantum number m with 95% accuracy. The application of perturbation theory to the $\mathbf{H}_0 \perp c$ data failed to properly account for the variation of $\Delta H_{\perp}$ with m, and the value of $g_{\perp}$ so obtained was recognized as being incorrect. Values of $g_{\perp}$ and B were therefore extracted from the experimental data by computing numerical solutions to the 24×24 secular equation, determining the field dependence of the hyperfine energy levels, and varying $g_{\perp}$ and B until the predicted positions of the hyperfine lines agreed with the experimental positions at an accurately known microwave frequency. The values of $g_{\parallel}$, D, and A were checked in this manner and found to be in excellent agreement with the perturbation theory results.

The final values of the spin-Hamiltonian parameters are given in Table I. These were obtained by comparing the eigenvalues of the 24×24 Hamiltonian matrix of Eq. (1) (determined within an $S=1$, $I=\frac{7}{2}$ manifold of spin states) with accurately determined field and frequency data for each hfs line measured at the turning points of the spectrum.

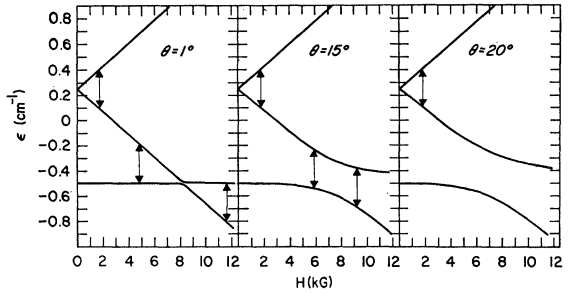

FIG. 4. Energy levels versus magnetic field for $S=1$. The arrows indicate resonant transitions at 9.3 GHz. All three transitions are observed at small angles. As θ increases the two high-field bands approach one another as the separation of the energy levels becomes larger, and finally for $\theta>16°$ these bands are no longer observed.

V. NATURE OF PARAMAGNETIC CENTER

The spin-Hamiltonian parameters show that the center has $S=1$ and $I=\frac{7}{2}$. The additional hfs lines of Fig. 3 were found to be due to normally forbidden $\Delta m=\pm 1, \pm 2$, and ± 3 nuclear transitions made allowed at intermediate angles by the mixing of spin states due to the large zero-field splitting. The 15 hfs lines of weak

TABLE I. Values of the spin-Hamiltonian parameters.

Parameter	Value	Estimated error
D/hc	± 0.7463 cm^{-1}	± 0.001 cm^{-1}
$g_{\parallel}$	1.9451	± 0.0005
$g_{\perp}$	1.9328	± 0.0005
A/hc	$\pm 66.1\times 10^{-4}$ cm^{-1}	$\pm 0.5\times 10^{-4}$ cm^{-1}
B/hc	$\pm 76.3\times 10^{-4}$ cm^{-1}	$\pm 0.5\times 10^{-4}$ cm^{-1}

intensity ($\Delta M=\pm 2$) observed at $\theta=20°$ are due to 8 $\Delta m=0$ lines plus 7 $\Delta m=\pm 1$ lines. A similar case of forbidden nuclear transitions for V^{2+} ($I=\frac{7}{2}$) may be found in the literature.[8] The absence of "unexplained" multiplicity of hyperfine structure shows that the isotope of the element giving rise to the paramagnetism must have nearly 100% natural abundance. Heat treatments also indicate thermal stability of the paramagnetic center over a wide temperature range. Considerations of all of the various possible ions with these characteristics led us to the conclusion that the paramagnetic center must be a V^{3+} ion. Emission- and mass-spectrographic analyses confirmed the presence of this element.

The EPR parameters for V^{2+} in ZnO have been measured.[9] The center is characterized by a ^4F ground state which is split by an axial field and spin-orbit coupling into two Kramers doublets. The spin is $S=\frac{3}{2}$, in contrast to $S=1$ for the V^{3+} case, and indicates one additional allowed transition at a given magnetic field. The anisotropic spectrum observed at 1.3°K and 9.1386 GHz showed an 8-line hyperfine structure. The spin-Hamiltonian parameters are $g_{\parallel}=1.977$, $g_{\perp}\simeq 2$, $D\simeq 0.3$ cm^{-1} and a hyperfine splitting of ~ 50 G. These values are quite different from those of V^{3+} in Table I.

The EPR data clearly showed that the center treated here has the same symmetry as a ZnO_4 tetrahedron in the ZnO crystal. However, a crystal defect associated with the V^{3+} ion and situated on the c axis would have the same symmetry. The spectrum was only found in crystals which were well compensated with monovalent impurities, as quantitative spectrographic analyses showed.

We have considered several models with axial interstitial atoms, axial substitutional atoms and axial vacancies, all having the required symmetry. In order to treat the magnetic properties of these models analytically, we consider the electrostatic potential of the ions surrounding the V^{3+} site, the most important part of which is the axial symmetry component. The total electrostatic potential is then considered as a pertubation on the quantum states of the two $3d$ electrons, which may be described by Hartree-Fock wave functions. Thus, our model completely neglects covalent interactions with the ZnO crystal.

VI. THEORY

For the $3d^2$ configuration of V^{3+}, the ground state is a ^3F which splits into $^3A_2$, $^3T_2$, and $^3T_1$ in a tetrahedral T_d crystalline field (Fig. 5). A trigonal C_{3v} component of the crystalline field further reduces the symmetry:

$$^3A_2\rightarrow {}^3A_2,\quad {}^3T_2\rightarrow {}^3A_1+{}^3E,\quad {}^3T_1\rightarrow {}^3A_2+{}^3E.$$

The other spin-triplet term within the $3d^2$ configuration

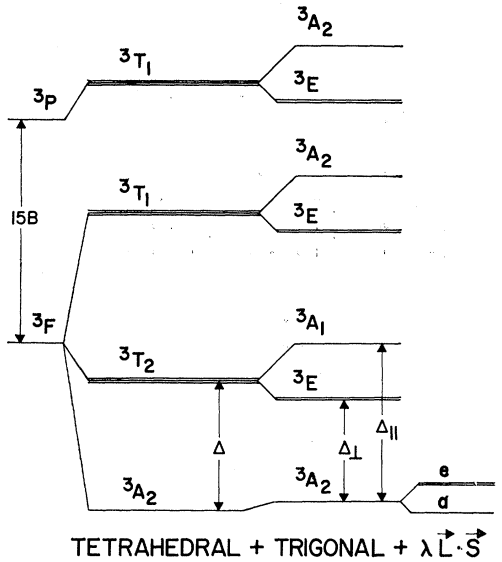

FIG. 5. Energy levels of ^3P and ^3F terms of $3d^2$ in a predominantly tetrahedral crystalline field. Further splitting is caused by a small trigonal distortion of tetrahedron and by spin-orbit coupling.

is ^3P which lies higher in energy than ^3F. The energy separation between these terms is due to the e^2/r_{12} interaction between the two $3d$ electrons, which is diagonal in the weak-field coupling scheme.[4] The ^3F-to-^3P separation is then 15 B, where B is the well-known Racah parameter.[4] The relative advantages of this scheme for the analysis of paramagnetism of V^{3+} have been discussed by Brumage, Quade, and Lin.[10]

The zero-field energy levels of $3d^2$ electrons of V^{3+} in ZnO are the eigenvalues of the equation

$$(\mathcal{H}_0+\mathcal{H}'+\mathcal{H}'')\phi=E\phi, \tag{2}$$

where $\mathcal{H}_0$ is the free-ion Hamiltonian excluding spin, $\mathcal{H}'$ is the contribution from the electrostatic crystal field, and $\mathcal{H}''$ accounts for spin-orbit coupling and the electronic spin-spin interactions.

The electrostatic effect on the electronic energy levels of V^{3+} by four point charges in C_{3v} symmetry, Fig. 1, is considered first. One electron cubic and axial crystal-field operators W_c and W_a are defined such that the operator for the C_{3v} charge configuration is given by

$$\mathcal{H}'=\sum_{i=1}^{2}[W_c(i)+W_a(i)]. \tag{3}$$

The operator for the tetrahedral-cubic potential[11] is well known[12]:

$$W_c=(\Delta/180)(O_4^0-20\sqrt{2}O_4^3), \tag{4}$$

[8] B. Bleaney and R. S. Rubins, Proc. Phys. Soc. (London) **77**, 103, (1961).
[9] T. L. Estle and M. DeWit, Bull. Am. Phys. Soc. 6, 445 (1961).
[10] W. H. Brumage, C. R. Quade, and C. C. Lin, Phys. Rev. **131**, 949 (1963).
[11] Equivalent operators valid within the ^3F term were found such that for $\mathcal{H}=H_c+H_a$, $H_c=\Delta(O_4^0-20\sqrt{2}O_4^3)/900$, and $H_a=DsO_2^0/15+DtO_4^0/60$.
[12] M. T. Hutchings, Solid State Phys. **16**, 227 (1964).

TABLE II. Cubic symmetry (T_d) basis functions for ^3F and ^3P.[a]

^3F

$^3A_2$: $\psi_0(^3A_2,M_s)=-\frac{1}{3}\sqrt{5}|0,M_s\rangle+\frac{1}{3}\sqrt{2}|3,M_s\rangle-|-3,M_s\rangle$

$^3T_2$: $\psi_1(^3T_2,M_s)=\frac{1}{2}\sqrt{2}(|3,M_s\rangle+|-3,M_s\rangle)$

$\psi_2(^3T_2,M_s)=\frac{1}{6}\sqrt{6}|-2,M_s\rangle+\sqrt{\frac{5}{6}}|1,M_s\rangle$

$\psi_3(^3T_2,M_s)=\frac{1}{6}\sqrt{6}|2,M_s\rangle-\sqrt{\frac{5}{6}}|-1,M_s\rangle$

$^3T_1$: $\psi_4(^3T_1,M_s)=\frac{2}{3}|0,M_s\rangle+\frac{1}{3}\sqrt{\frac{5}{2}}(|3,M_s\rangle-|-3,M_s\rangle)$

$\psi_5(^3T_1,M_s)=\sqrt{\frac{5}{6}}|-2,M_s\rangle-\frac{1}{6}\sqrt{6}|1,M_s\rangle$

$\psi_6(^3T_1,M_s)=\sqrt{\frac{5}{6}}|2,M_s\rangle+\frac{1}{6}\sqrt{6}|-1,M_s\rangle$

^3P

$\chi_1(^3T_1,M_s)=|1,M_s\rangle$

$\chi_2(^3T_1,M_s)=|0,M_s\rangle$

$\chi_3(^3T_1,M_s)=-|-1,M_s\rangle$

[a] The first number inside the ket $|\ \rangle$ refers to the value of M_L, the last to M_s. Apart from the symbols ψ_n and χ_n (bases for ^3F and ^3P, respectively) the remaining notation is standard.

where $\Delta=10Dq$ is given in the electrostatic approximation by

$$\Delta=(20/27)Ze^2\langle r^4\rangle/d^5. \tag{5}$$

The operator for the axial component of the electrostatic potential is found by considering the potential of a charge q located on the crystalline c axis at a distance a from the V^{3+} ion. With the origin of coordinates at the V^{3+} ion, we find

$$V(x,y,z)=q(x^2+y^2+z^2-2az)^{-1/2}.$$

We do a Taylor's-series expansion of this potential according to the prescription of Hutchings,[12] and compute the energy $W=-|e|V(x,y,z)$ of an electron in this potential field. The result is

$$W_a=-\frac{q|e|}{2a}\left(\frac{3z^2-r^2}{a^2}\right)-\frac{q|e|}{8a}\left(\frac{35z^4-30z^2r^2+3r^4}{a^4}\right). \tag{6}$$

This is next put into a convenient operator form by using the operator equivalents

$$3z^2-r^2=a\langle r^2\rangle O_2^0,$$

$$35z^4-30z^2r^2+3r^4=\beta\langle r^4\rangle O_4^0,$$

where for one d electron $\alpha=-2/21$, $\beta=+2/63$. For convenience in calculation, we use the standard Ds, Dt notation for the coefficients of $\frac{1}{3}O_2^0$ and $\frac{1}{12}O_4^0$, respectively, so that W_a becomes (after allowing for a specific charge redistribution)

$$W_a=\tfrac{1}{3}DsO_2^0-\tfrac{1}{12}DtO_4^0. \tag{7}$$

In introducing these symbols, we have taken care to be consistent with existing conventions. These symbols were originally introduced by Ballhausen and Moffitt,[13] and a similar electrostatic model for a tetragonally distorted octahedron has been worked out by Piper and Carlin.[14] Specific expressions for Ds and Dt are given in Sec. VII.

The spin-orbit coupling and the electronic spin-spin interactions are the remaining zero-field perturbations

$$\mathcal{H}''=\sum_{i=1}^{2}\{\xi\mathbf{l}_i\cdot\mathbf{s}_i\}+W_{ss}.$$

The spin-orbit operator may be replaced by $\lambda\mathbf{L}\cdot\mathbf{S}$ within a term, where $\lambda=\frac{1}{2}\xi$ for both ^3P and ^3F. The spin-spin magnetic dipolar interaction was only considered within the ^3F term. The equivalent operator

$$W_{ss}=-\rho\{(\mathbf{L}\cdot\mathbf{S})^2+\tfrac{1}{2}\mathbf{L}\cdot\mathbf{S}-\tfrac{1}{3}L(L+1)S(S+1)\}$$

was used. Pryce[15] has given for ρ of V^{3+} $3d^2$ ^3F, the value $\rho=0.24\pm0.05$ cm^{-1}. The resulting contribution to D is less than 0.01 cm^{-1}, so W_{ss} was completely neglected in further calculations.

The effect of the crystal field on the orbital energy levels was evaluated using the operators of Eqs. (3)–(7) operating on the symmetrized combinations of basis functions[16] listed in Table II. The resulting matrix elements are given in Table III. These matrix elements were found to be identical to those of Brumage *et al.*[10] who, however, used a nonstandard notation in their calculations. The matrix elements of the spin-orbit coupling, were then determined using the 30 basis kets of the sets $\{\psi_n\otimes|1,M_s\rangle\}$ and $\{\chi_n\otimes|1,M_s\rangle\}$. This gave a final 30×30 dimension Hamiltonian matrix which de-

TABLE III. Matrix elements of the crystal-field operators W_c and W_t in cubic (T_d) representation.

$^3A_2(^3F)$

$\langle\psi_0\|\psi_0\rangle=-12Dq+\frac{1}{3}14Dt$

$^3T_2(^3F)$

$\langle\psi_1\|\psi_1\rangle=-2Dq+Ds+3Dt$

$\langle\psi_2\|\psi_2\rangle=-2Dq-\frac{1}{2}Ds-\frac{1}{3}Dt$

$\langle\psi_3\|\psi_3\rangle=\langle\psi_2\|\psi_2\rangle$

$^3T_1(^3F)$

$\langle\psi_4\|\psi_4\rangle=+6Dq+\frac{1}{5}Ds+\frac{1}{3}13Dt$

$\langle\psi_5\|\psi_5\rangle=+6Dq-\frac{1}{10}Ds-\frac{1}{3}17Dt$

$\langle\psi_6\|\psi_6\rangle=\langle\psi_5\|\psi_5\rangle$

$^3T_1(^3P)$

$\langle\chi_2\|\chi_2\rangle=15B+\frac{1}{5}14Ds$

$\langle\chi_1\|\chi_1\rangle=15B-\frac{1}{5}7Ds$

$\langle\chi_3\|\chi_3\rangle=\langle\chi_1\|\chi_1\rangle$

$^3T_1(^3F)$ coupling to $^3A_2(^3F)$

$\langle\psi_0\|\psi_4\rangle=2Ds/\sqrt{5}-2\sqrt{5}Dt/3$

$^3T_1(^3F)$ coupling to $^3T_2(^3F)$

$\langle\psi_2\|\psi_5\rangle=\langle\psi_3\|\psi_6\rangle=Ds/2\sqrt{5}-4\sqrt{5}Dt/3$

$^3T_1(^3P)$ coupling to $^3A_2(^3F)$

$\langle\psi_0\|\chi_2\rangle=-4Ds/\sqrt{5}+4\sqrt{5}Dt/3$

$^3T_1(^3P)$ coupling to $^3T_2(^3F)$

$\langle\psi_2\|\chi_1\rangle=\langle\psi_3\|\chi_3\rangle=4Ds/\sqrt{5}+\sqrt{5}Dt$

$^3T_1(^3P)$ coupling to $^3T_1(^3F)$

$\langle\psi_4\|\chi_2\rangle=4Dq+\frac{1}{5}8Ds-\frac{1}{3}8Dt$

$\langle\psi_5\|\chi_1\rangle=\langle\psi_6\|\chi_3\rangle=4Dq-\frac{1}{5}4Ds-Dt$

[13] C. J. Ballhausen and W. Moffitt, J. Inorg. Nucl. Chem. **3**, 178 (1956).

[14] T. S. Piper and R. L. Carlin, J. Chem. Phys. **33**, 1208 (1960).

[15] M. H. L. Pryce, Phys. Rev. **80**, 1107 (1950).

[16] S. A. Al'tshuler and B. M. Kozyrev, *Electron Paramagnetic Resonance* (Academic Press Inc., New York, 1964).

termines the zero-field energy levels in the electrostatic approximation.

The perturbation formulas of Abragam and Pryce[17] were used as a first approximation for the spin-Hamiltonian parameters as functions of Dq, Ds, Dt, and λ. The results are

$$g_{\parallel}=g_e-8\lambda/\Delta_{\parallel}, \tag{8a}$$

$$g_{\perp}=g_e-8\lambda/\Delta_{\perp}, \tag{8b}$$

$$D=4\lambda^2(1/\Delta_{\perp}-1/\Delta_{\parallel}), \tag{8c}$$

$$A=-P(\kappa+8\lambda/\Delta_{\parallel}), \tag{8d}$$

$$B=-P(\kappa+8\lambda/\Delta_{\perp}). \tag{8e}$$

In these equations, $\Delta_{\parallel}$ and $\Delta_{\perp}$ follow as the differences ${}^3A_1-{}^3A_2$ and ${}^3E-{}^2A_2$ of the diagonal matrix elements in Table III,

$$\begin{aligned}\Delta_{\parallel}&=\Delta'+2(\tfrac{1}{2}Ds+\tfrac{1}{9}10Dt),\\ \Delta_{\perp}&=\Delta'-(\tfrac{1}{2}Ds+\tfrac{1}{9}10Dt),\\ \Delta'&=\Delta-\tfrac{1}{9}35Dt=\tfrac{1}{3}(\Delta_{\parallel}+2\Delta_{\perp}).\end{aligned} \tag{9}$$

The gyromagnetic ratio of the free electron is $g_e=2.002322$. A value for P for V^{3+} can be found by reference to McGravey's paper on the isotropic hyperfine interaction[18]: $P=150\times10^{-4}$ cm^{-1}. The quantity κP should be a property of the V^{3+} ion, if covalent effects do not greatly affect the S-electron spin density at the nucleus. We deduced a value for κP from the g value and hyperfine constant A of the isotropic EPR spectrum of V^{3+} in ZnS.[1] The value $\kappa P=-54.15\times10^{-4}$ cm^{-1} was found, on the assumption that A for ZnS:V^{3+} is negative.

The three equations, (8a), (8b), and (8c), were used to determine the three unknowns, λ, $\Delta_{\parallel}$, $\Delta_{\perp}$ and the results are shown in Table IV. According to these equations, the values of λ, $\Delta_{\parallel}$, and $\Delta_{\perp}$ are independent of Δ. This is unreasonable from a physical point of view. In addition, $\lambda>\lambda_0$ which is unusual, and warrented further investigation.

More accurate equations for the spin-Hamiltonian parameters were therefore derived in an attempt to resolve the peculiarities found in the first-order equations. The spin-Hamiltonian parameters were found from these operator relations which were derived for an electronic spin $S=1$ system.

$$g_{\parallel}=\langle e|L_z+g_eS_z|e\rangle \tag{10a}$$

$$g_{\perp}=\langle a|L_x+g_eS_x|e\rangle, \tag{10b}$$

$$D=E(e)-E(a), \tag{10c}$$

$$\begin{aligned}A=P\langle e|&L_z+(4/35-\kappa)S_z\\&-(1/70)(\mathbf{L}\cdot\mathbf{S})L_z-(1/70)L_z(\mathbf{L}\cdot\mathbf{S})|e\rangle,\end{aligned} \tag{10d}$$

$$\begin{aligned}B=2^{-1/2}P\langle a|&L_x+(4/35-\kappa)S_x\\&-(1/70)(\mathbf{L}\cdot\mathbf{S})L_x-(1/70)L_x(\mathbf{L}\cdot\mathbf{S})|e\rangle.\end{aligned} \tag{10e}$$

[17] A. Abragam and M. H. L. Pryce, Proc. Roy. Soc. (London) **A205**, 135 (1951).
[18] B. R. McGarvey, J. Phys. Chem. **71**, 51 (1967).

TABLE IV. Solutions to Eqs. (8a)–(8c) and (9) for several values of Δ.

Δ cm^{-1}	Ds cm^{-1}	Dt cm^{-1}	λ cm^{-1}	$\Delta_{\parallel}$ cm^{-1}	$\Delta_{\perp}$ cm^{-1}
11 000	4269	−1019	121	16 965	13 963
12 500	3414	−634	121	16 965	13 963
13 000	3124	−505	121	16 965	13 963
14 000	2554	−248	121	16 965	13 963
15 000	1984	9	121	16 965	13 963
15 600	1634	164	121	16 965	13 963

The kets $|a\rangle$ and the doubly degenerate set $|e_{+1}\rangle$ and $|e_{-1}\rangle$ were then found in the second-order perturbation approximation as

$$|e_1\rangle=N_e\left[|\psi_0,1\rangle-\frac{2\lambda}{\Delta_{\parallel}}|\psi_1,1\rangle+\frac{2\lambda}{\Delta_{\perp}}|\psi_2,0\rangle-\frac{K}{\Delta_2}|\psi_4,1\rangle\right],$$

$$\begin{aligned}|a\rangle=N_a\Big[&|\psi_0,0\rangle+\frac{2\lambda}{\Delta_{\perp}}|\psi_2,-1\rangle\\&-\frac{2\lambda}{\Delta_{\perp}}|\psi_3,1\rangle-\frac{K}{\Delta_2}|\psi_4,0\rangle\Big],\end{aligned}$$

$$\begin{aligned}|e_{-1}\rangle=N_e\Big[&|\psi_0,-1\rangle+\frac{2\lambda}{\Delta_{\parallel}}|\psi_1,-1\rangle\\&-\frac{2\lambda}{\Delta_{\perp}}|\psi_3,0\rangle-\frac{K}{\Delta_2}|\psi_4,-1\rangle\Big].\end{aligned}$$

The new parameters which we have introduced here are

$$\Delta_2=\tfrac{1}{5}9\Delta+\tfrac{1}{5}Ds-\tfrac{1}{3}Dt,$$

$$K=\tfrac{2}{5}\sqrt{(5)}Ds-\tfrac{2}{3}\sqrt{(5)}Dt,$$

$$N_e=\left(1+\frac{4\lambda^2}{\Delta_{\parallel}^2}+\frac{4\lambda^2}{\Delta_{\perp}^2}+\frac{K^2}{\Delta_2^2}\right)^{-1/2},$$

$$N_a=\left(1+\frac{8\lambda^2}{\Delta_{\perp}^2}+\frac{K^2}{\Delta_2^2}\right)^{-1/2}.$$

The resulting expressions for the spin-Hamiltonian parameters were found to be

$$\begin{aligned}g_{\parallel}=N_e^2\Big(g_e\Big(&1+\frac{4\lambda^2}{\Delta_{\parallel}^2}+\frac{K^2}{\Delta_2^2}\Big)\\&-\frac{8\lambda}{\Delta_{\parallel}}+\frac{4\sqrt{(5)}K}{\Delta_2\Delta_{\parallel}}+\frac{2\lambda^2}{\Delta_{\perp}^2}\Big),\end{aligned} \tag{11a}$$

$$\begin{aligned}g_{\perp}=N_eN_a\Big(g_e\Big(&1+\frac{4\lambda^2}{\Delta_{\perp}^2}+\frac{K^2}{\Delta_2^2}\Big)\\&-\frac{8\lambda}{\Delta_{\perp}}-\frac{2\sqrt{(5)}K\lambda}{\Delta_2\Delta_{\perp}}+\frac{2\lambda^2}{\Delta_{\parallel}\Delta_{\perp}}\Big),\end{aligned} \tag{11b}$$

$$D=4\lambda^2\left(\frac{1}{\Delta_{\perp}}-\frac{1}{\Delta_{\parallel}}\right). \tag{11c}$$

TABLE V. Solutions to Eqs. (11) for several values of Δ.[a]

	Δ cm^{-1}	Ds cm^{-1}	Dt cm^{-1}	λ cm^{-1}	A-B cm^{-1} ×10^4	$\Delta_{\parallel}$ cm^{-1}	$\Delta_{\perp}$ cm^{-1}
D	10 000	1677	−1486	134	13.2	14 154	16 592
Negative	11 000	1820	−1561	145	12.9	15 422	17 895
	12 000	1980	−1635	155	12.6	16 705	19 185
D	11 000			no solution			
Positive	12 500	−890	1339	59	−5.5	9 378	6 250
	13 000	−444	1139	69	−3.4	10 824	7 527
	14 000	45	913	84	−1.2	12 523	9 413
	15 000	376	756	97	0.2	14 116	11 032
	15 600	541	678	104	0.7	15 011	11 940

[a] The value of P given in the text was used in the calculation of A-B.

Eliminating the smaller terms in the equations for A and B

$$A=P\left(-\kappa+g_{\parallel}-g_e+\frac{4\sqrt{(5)}K}{35\Delta_2}\right), \tag{12a}$$

$$B=P\left(-\kappa+g_{\perp}-g_e-\frac{2\sqrt{(5)}K}{35\Delta_2}\right), \tag{12b}$$

and

$$A-B=P\left(g_{\parallel}-g_{\perp}+\frac{6\sqrt{(5)}K}{35\Delta_2}\right). \tag{12c}$$

VII. DISCUSSION

Solutions for Eqs. (11a)–(11c) were obtained using the experimental data of Table I. A reiterative computer program was used which required an input value of Δ and found values of Ds, Dt, and λ which satisfied all three nonlinear equations. Both signs of D were considered and the results are listed in Table V. Since we now have four variables and three equations, we needed some additional criteria for selecting a solution. These criteria are: Ds and Dt should both be of the same sign and λ should be less than or equal to $\lambda_0=104$ cm^{-1} (free ion). It was found possible to satisfy these criteria as Table V shows, for the values of Δ in the range 14 000–15 600 cm^{-1}. The reasons for applying the criteria will be discussed later.

A comparison of the results using the first-order equations, Table IV, and the higher-order equations, Table V, were made for several values of Δ. For the first-order equations, it is important to note that λ, $\Delta_{\parallel}$, and $\Delta_{\perp}$ are independent of the value of Δ. This physically unrealistic situation does not occur with the higher-order equations. Thus, a value of Δ must be chosen in order to determine λ, Ds, and Dt. Usually a value of Δ is obtained from optical measurements. This was not possible due to the low vanadium concentrations, so approximate values of Δ were used.

Another feature of the higher-order equations is that values of λ lower than λ_0, are possible because λ is a function of Δ. This is not the case with the results from the first-order equations.

The higher-order terms in Eqs. (11a) and (11b) are frequently small in relation to the first-order term $8\lambda/\Delta_{\parallel}$. Some of the terms such as $2\lambda^2/\Delta_{\perp}^2$ and $4\lambda^2/\Delta_{\parallel}^2$ are smaller, for some values of Δ, than the experimental error in the g factors and could be neglected to a good approximation. They were retained, however, for the computer calculations. The magnitude of the terms containing K for some values of Δ may also be relatively small. For example, using $\Delta=15\,600$ cm^{-1} the largest higher-order term in the Eq. (11a) is $4\sqrt{(5)}K/\Delta_2\Delta_{\parallel}$ and it is ∼2% of the value of the first-order term $8\lambda/\Delta_{\parallel}$. Despite the relatively small value of the higher-order terms in this example, these terms do introduce the parameter Δ and because of the presence of these terms in the equations, an average decrease of ∼16% in λ, $\Delta_{\parallel}$, and $\Delta_{\perp}$ is produced. Using other values of Δ, the correction between the first-order and higher-order equations becomes even greater as noted from Table V, e.g., at 15 000 cm^{-1} an average decrease of ∼25% occurs.

One of the criteria for selecting a value of Δ is that both Ds and Dt have the same sign. In ZnO the deviation from tetragonal symmetry is principally the result of the elongation of the Zn-O bond along the Z axis direction (Fig. 1). The electrostatic effect of this distortion may be treated by the use of Eq. (6). The effective oxide charge $-Z|e|$ at distance "d" (of a tetrahedron) is removed and replaced by a charge $-Z|e|$ at distance "a" along the Z axis. The resulting operator is then put into the form of Eq. (7). The resulting expressions for Ds and Dt are

$$Ds=(1/7)Ze^2\langle r^2\rangle(1/d^3-1/a^3), \tag{13a}$$

$$Dt=(1/21)Ze^2\langle r^2\rangle(1/d^5-1/a^5). \tag{13b}$$

For cubic symmetry, $a=d$ and $Ds=Dt=0$, as required.

According to Eqs. (13), Ds and Dt always have the same sign and for $a>d$ (according to the latest crystallographic data)[7] Ds and Dt are both positive. Studies of the optical spectra of an analogous system ($3d^8$ in tetragonally distorted sixfold octahedral symmetry) which also use the electrostatic model have shown that the off-diagonal matrix elements of Ds and Dt are very important. The experimental values of Ds and Dt in a study of 12 inorganic crystalline compounds of Ni^{2+} were found to always be of the same sign.[19] Piper and Carlin[14] showed that for $Al_2O_3:V^{3+}$ Ds and Dt calculated by the use of electrostatic approximation including known trigonal distortion were both positive and their values agreed well with the experiment. It is for these reasons that we require that acceptable solutions to Eqs. (11) have Ds and Dt of the same sign. This sets a lower limit of ∼14 000 cm^{-1} for Δ.

A second criterion used is to select a value of Δ for which $\lambda<\lambda_0$. Experimentally, it is generally observed that $\lambda<\lambda_0$ in solids,[20] although there appears to be no fundamental reason why this must be the case.[21] Gen-

[19] R. A. Rowley and R. S. Drago, Inorg. Chem. 1, 795 (1968).
[20] M. Gerloch and J. R. Miller, Progr. Inorg. Chem. 10, 1 (1968).
[21] G. Weber, Z. Physik 190, 135 (1966).

erally, λ decreases from the free-ion value as the covalency increases. Brumage, Quade, and Lin[10] have found after a careful study of the paramagnetic susceptibility of $Al_2O_3:V^{3+}$ that $\lambda(V^{3+})=95\pm5$ cm^{-1}. This criterion ($\lambda\leq\lambda_0$) sets an upper limit of 15 600 cm^{-1} to the value of Δ.

Several additional results agree with a value of Δ in the 14 000–15 600 cm^{-1} range. The calculated value of A-B using Eq. (12c) is positive for $\Delta\gtrsim15\,000$ as seen from Table V assuming both A and B are negative.[18] Experimentally A-B is also positive as seen from Table I, assuming both A and B are negative. The absolute values of both A and B are smaller, however, than the experimental values using a value of P determined for $ZnS:V^{3+}$.

An estimate of the value of Δ was obtained by considering the isotropic g values for V^{3+} in the crystals ZnS, ZnTe, and CdS, mentioned in the Introduction. These g values are related to λ and Δ by the approximation

$$g=g_e-8\lambda/\Delta.$$

We can find an average isotropic g value for $ZnO:V^{3+}$ as $\langle g\rangle=\frac{1}{3}(g_{\parallel}+2g_{\perp})=1.9369$. Now λ depends on the covalency of the crystal; as the covalency increases, then λ generally decreases. If we plot oxygen-metal distance "d" versus λ, and assume a linear dependence where $\lambda\simeq\lambda_0$ for ZnO and $\lambda\simeq0.75\lambda_0$ for ZnTe, then we can calculate Δ for ZnS, CdS, ZnTe. When Δ is plotted versus d, and extrapolated to $d=1.978$ Å for ZnO, a value of $\Delta>15\,000$ cm^{-1} was obtained. This is consistent with the range of Δ values determined here for $ZnO:V^{3+}$.

The approximate values of Ds and Dt for V^{3+} in a Zn^{++} site were next estimated. In order to do this, we need approximate values for the averages $\langle r^2\rangle$ and $\langle r^4\rangle$. The approximate Hartree-Fock–type radial functions of Richardson *et al.*[22] were used for this purpose. The results were $\langle r^2\rangle=1.768\,a_0^2$, $\langle r^4\rangle=6.919a_0^4$, and $\langle r^2\rangle/\langle r^4\rangle=0.255/a_0^2$. We avoid use of the absolute values of $\langle r^n\rangle$ by using only the ratio $\langle r^2\rangle/\langle r^4\rangle$ wherever possible. Ds and Dt for the axially elongated tetrahedron were estimated by using a value of $\Delta=15\,600$ cm^{-1} and Eq. (5); this determines $Ze^2\langle r^4\rangle$. Then Ds and Dt are found from Eqs. (13) and the above values of $\langle r^2\rangle/\langle r^4\rangle$. The results are $Ds=+291$ cm^{-1}, $Dt=+45$ cm^{-1}. After a consideration of the errors involved in neglecting higher-energy states and in using perturbation theory,[23] the values of Ds and Dt determined using the higher-order equations are of the same sign and within an order of magnitude of the value of Ds and Dt determined using Eq. (13).

TABLE VI. Values of $\Delta=10Dq$ for V^{3+} in octahedral and tetrahedral coordination and for other ions in ZnO.

System	$\Delta=10Dq$ (cm^{-1})	Comments
$CsAlCl_4:V^{3+}$	8 800	Tetrahedral[a]
$Al_2O_3:V^{3+}$	17 500	Trigonally distorted octahedral[b]
	19 050	c
$6H_2O:V^{3+}$	18 600	d
$ZnO:Cu^{2+}$	5 690	Trigonally distoretd tetrahedral[e]

[a] R. M. Gruen and R. Gut, Nature **190**, 713 (1961).
[b] M. H. L. Pryce and W. A. Runciman, Disc. Faraday Soc. **26**, 34 (1958).
[c] See Ref. 10.
[d] Y. Tanabe and S. Sugano, J. Phys. Soc. Japan **9**, 766 (1954).
[e] R. E. Dietz, H. Kamimura, M. D. Sturge, and A. Yariv, Phys. Rev. **132**, 1559 (1963).

A cubic field splitting for the range of Δ satisfying our criteria is larger than one might expect from comparisons of the optical spectra of V^{3+} in other crystals (see Table VI), keeping in mind the empirical rules[24] that Δ(octahedral, sixfold coordinated)$\approx-\frac{1}{4}9\Delta$ (tetrahedral) and $\Delta(M^{3+})\approx\frac{3}{2}\Delta(M^{2+})$. Thus, from these rules and Table VI one would anticipate a value for Δ (V^{3+}, tetrahedral)$\approx$8500 cm^{-1}. However, this must be corrected for the fact that V^{3+} is now substitutional for a Zn^{2+} in a divalent lattice, for which some slight compression of the tetrahedron of atoms about the V^{3+} is to be expected. Now, Drickamer[25] has shown that the crystal-field parameter $\Delta=10\,Dq$ for V^{3+} ions in MgO and Al_2O_3 varies versus pressure as Eq. (5) predicts, i.e., $d(Dq)/dp\sim d^{-5}$. Then, for an order of magnitude calculation, let the cubic d (ZnO)$=1.978$ Å. A 0.1 Å compression of the tetrahedron (a value which we found reasonable for the compression caused by an extra positive charge) gives Δ (compressed)$\approx11\,000$ cm^{-1}, in closer agreement with the Δ which satisfies our criteria.

In summary, the higher-order equations have terms which make the values of λ, $\Delta_{\parallel}$, and $\Delta_{\perp}$ dependent on the value of Δ and they make it possible to obtain values of $\lambda<\lambda_0$ Both situations are physically realistic. This is not the case with the first-order equations. In addition, the difference in the magnitude of these parameters as determined from the first-order and higher-order equations can be significant.

This analysis was made using an electrostatic model, which is a reasonable approach in view of the ionic character of ZnO compared to the other II-VI compounds. Using the higher-order equations and the imposed criteria, a range of Δ values of 14 000–15 600 cm^{-1} was selected. The values in this range are in agreement with a positive difference between A and B, with an extrapolated Δ value obtained by considering the variation of Δ with covalency in other II-VI compounds,

[22] J. W. Richardson, W. C. Nieuwpoort, R. R. Powell, and W. F. Edgell, J. Chem. Phys. **36**, 1057 (1962).

[23] The magnitude of the error involved when neglecting the ^3P state and in using the cubic field diagonal energies for Δ_2, $\Delta_{\parallel}$, $\Delta_{\perp}$ was obtained for the case of $\Delta=15\,600$ cm^{-1}, The matrix equation (3) was diagonalized using $15B=10\,000$ cm^{-1}, $\Delta=15\,600$ cm^{-1} and various values of Ds and Dt. The eigenvalues were then used to obtain the corrected values for Δ_2, $\Delta_{\parallel}$, $\Delta_{\perp}$. Using these corrected values in Eqs. (11), we found $g_{\parallel}$ and $g_{\perp}$. The new values of Ds and Dt which satisfied these equations were in the range of 100 cm^{-1} below the approximate solution of $Ds=541$ cm^{-1} and $Dt=678$ cm^{-1}. Since neither $15B$ nor Δ could be obtained experimentally, the improved accuracy of the values of Ds and Dt obtained using this more involved computation was not considered fruitful at this time.

[24] P. George and D. S. McClure, Progr. Inorg. Chem. **1**, 381 (1959).

[25] S. Minomura and H. G. Drickamer, J. Chem. Phys. **35**, 903 (1961).

and with recent crystallographic data on ZnO. This range is higher than the 8500–11 000 cm^{-1} range which was estimated from optical data on V^{3+} in other crystals using some empirical rules and a contracted tetrahedron.

We attribute the source of this discrepancy, between expected and deduced values of Δ, to the neglect of covalency in the electrostatic model. As long ago shown by Owen,[26] covalency appears in the equations for the magnetic properties of a metal complex as an anisotropic spin-orbit coupling. This effect was later investigated in more detail by Kamimura,[27] to whose paper we refer for a description of covalent anisotropic coupling for a spin $S \geq 1$ system. The empirical introduction of this effects into our treatment leads to more unknowns than we can evaluate. Likewise, a self-consistent-field calculation based on linear combinations of atomic orbitals for molecular orbitals would lead to still more unknown parameters, so for this reason the covalent model was not pursued.

Some consideration was given to the possibility of a Li^+ atom, or a Zn^{++} vacancy at the next-nearest c-axis Zn site. The nearest-neighbor effects are expected to be well described by an electrostatic model because of the short-range nature of covalent overlap and the large distance (5.207 Å) between Zn^{++} sites along the c axis. For an effective charge of q' at distance d' along the c axis we find

$$Ds = q'|e|\langle r^2\rangle/7\epsilon(d')^3,$$
$$Dt = q'|e|\langle r^4\rangle/21\epsilon(d')^5.$$

The effective charge $q' \approx -|e|$ for a Li^+ ion and $q' \approx -2|e|$ for a Zn^{++} vacancy. The dielectric shielding constant $1 \leq \epsilon \leq \epsilon_0$ is introduced in order to account for the reduction of the potential at V^{3+} due to the polarizability of the oxygen atom lying between the V^{3+} and the axial charge q'. These contributions to Ds and Dt are found to be much smaller and of opposite sign in comparison to Ds and Dt of the naturally elongated ZnO_4 tetrahedron of the ZnO crystal. Therefore, an associated positive ion such as Li^+ or Na^+ could be present at the nearest-neighbor c-axis Zn^{++} site, since this is not inconsistent with our analysis of the EPR data. The binding energy of a V^{3+}-O-M^+ pair of metal ions would help to explain the stability of this center, which remained stable up to high temperatures under conditions intended to reduce V^{3+} to V^{2+}. Charge neutrality arguments, however, only require that compensating M^+ charges exist somewhere in the crystal, not necessarily in a next-neighbor site.

[26] J. Owen, Proc. Roy. Soc. (London) **A227**, 183 (1955).
[27] H. Kamimura, Phys. Rev. **128**, 1077 (1962).

VIII. CONCLUSIONS

A vanadium ion in a $3d^2$ configuration has been identified in single crystals of ZnO by the EPR method. The spin-Hamiltonian parameters were accurately determined. These parameters were interpreted using an electrostatic model and the weak-field coupling scheme. A model in which V^{3+} is substitutional for a Zn atom and is surrounded by four oxygen atoms was found to give good agreement with experimental results. Our model agrees with the most recently determined atomic distances in ZnO[7] in which one of the oxygen-vanadium distances is slightly elongated. The analysis of the EPR data does not preclude that this V^{3+} center may be thermally stabilized by an associated monovalent metal ion.

ACKNOWLEDGMENTS

Sustained encouragement by Dr. O. N. Salmon, Manager, Solid State Physics Research and assistance by E. B. Aus in all phases of experimental work are gratefully acknowledged. We are also indebted to Dr. D. H. Hogle of the Dielectric Materials and Systems Laboratory for providing the crystals, to Dr. E. L. Cook for help with computations, to Dr. G. E. Gurr for bringing to our attention new crystallographic data on ZnO and to members of Analytical Research and Services Laboratory: for emission spectroscopy, J. A. Leys, for x-ray diffraction analyses, Dr. W. E. Thatcher. We are grateful to Professor J. E. Wertz and Professor J. R. Bolton of the University of Minnesota for the use of their Magnetic Resonance equipment at some stages of experimental work.